Inorg. Chem. **2007**, *46*, 2914–2920

Inorganic Chemistry
Article

Tetrahedral D Atom Coordination of Nickel and Evidence for Anti-isostructural Phase Transition in Orthorhombic $Ce_2Ni_7D_{\sim 4}$

Yaroslav E. Filinchuk,*,†,‡ Klaus Yvon,† and Herman Emerich‡

Laboratory of Crystallography, University of Geneva, 24 quai Ernest Ansermet, CH-1211 Geneva, Switzerland, and Swiss-Norwegian Beam Lines at European Synchrotron Radiation Facility (ESRF), BP-220, F-38043 Grenoble, France

Received December 4, 2006

Hydrogenation of hexagonal Ce_2Ni_7 was investigated by synchrotron X-ray and neutron powder diffraction. In contrast to the recently investigated lanthanum analogue, which remains hexagonal ($La_2Ni_7D_{6.5}$: space group $P6_3/mmc$), the cerium compound becomes orthorhombic ($Ce_2Ni_7D_{\sim 4}$: space group *Pmcn*). As in the structurally related $CeNi_3D_{2.8}$, deuterium occupies $CeNi_2$ slabs only, while the bulk of the $CeNi_5$ slabs remains empty. A significant amount of deuterium is bonded in tetrahedral NiD_4 units similar to those in nickel-based complex metal hydrides. These findings provide further evidence for directional bonding effects in hydrides that are traditionally considered as "interstitial". $Ce_2Ni_7D_{\sim 4}$ displays various orthorhombic lattice distortions, $\delta = (b/\sqrt{3} - a)/a$. Hydrogen pressures of ~30 bar stabilize a phase having a negative distortion ($\delta < 0$). Upon a decrease in the pressure, this phase transforms via a two-phase region into another phase having a positive distortion ($\delta > 0$). Both phases are nearly isostructural and have the same space group symmetry and nearly the same composition. This situation is typical for a so-called anti-isostructural phase transition in which δ is considered to be an order parameter. Neither magnetic nor structural transitions have been detected down to 1.5 K.

1. Introduction

Because of their superior properties for applications in rechargeable metal hydride batteries, intermetallic compounds of composition R_2T_7 and RT_3 (R = rare earth; T = transition element) and their hydrides are of renewed interest.[1] The compounds occurring in the Ce−Ni system have closely related but distinctly different crystal structures. Ce_2Ni_7 crystallizes in its own structure type.[2] It contains two sorts of structural slabs that alternate along the hexagonal axis, one consisting of double layers of $CeNi_5$ (a fragment of $CaCu_5$ type structure) and the other of double layers of $CeNi_2$ (a fragment of $MgCu_2$ type structure). $CeNi_3$ is closely related to Ce_2Ni_7, except that it contains single, not double, layers in the $CeNi_5$ slabs. Both compounds react easily with hydrogen and form so-called "interstitial" hydrides, of which one ($CeNi_3D_{2.8}$) has been fully structurally characterized.[3] Striking aspects of both hydrides are their equilibrium pressures, structural distortions, and H atom distributions. For $CeNi_3H_2$, the equilibrium pressure was reported to be 0.1 bar at 50 °C.[4] Upon hydrogenation, the structure of $CeNi_3$ undergoes an anomalous expansion along the hexagonal *c* axis (~30%) and a small contraction in the basal plane.[4,5] As shown by a recent neutron powder diffraction (NPD) study,[3] the deuteride $CeNi_3D_{2.8}$ has an orthorhombic distorted structure in which eight D atom sites fill exclusively $CeNi_2$ slabs, with the $CeNi_5$ slabs remaining empty. Furthermore, in contrast to most other "interstitial" hydrides, some of the H atoms do not fill interstices that exist in the intermetallic compound but occupy newly created ones. This anomaly cannot be explained by the interstitial concept. Ce_2Ni_7 shows a very similar behavior. The equilibrium pressure of its nearly stoichiometric hydride $Ce_2Ni_7H_{\sim 4}$ is 0.2 bar at 50 °C,[4] i.e., only slightly higher than that of $CeNi_3H_{2.8}$.

* To whom correspondence should be addressed. E-mail: Yaroslav.Filinchuk@esrf.fr. Tel: +33-476-88-2775. Fax: +33-476-88-2694.
† University of Geneva.
‡ ESRF.

(1) Yasuoka, S.; Magari, Y.; Murata, T.; Tanaka, T.; Ishida, J.; Nakamura, H.; Nohma, T.; Kihara, M.; Baba, Y.; Teraoka, H. *J. Power Sources* **2006**, *156*, 662−666.
(2) Cromer, D. T.; Larson, A. C. *Acta Crystallogr.* **1959**, *12*, 855−859.
(3) Yartys, V. A.; Isnard, O.; Riabov, A. B.; Akselrud, L. G. *J. Alloys Compd.* **2003**, *356−357*, 109−113.
(4) van Essen, R. H.; Buschow, K. H. J. *J. Less-Common Met.* **1980**, *70*, 189−198.
(5) Burnasheva, V. V.; Tarasov, B. P.; Semenenko, K. N. *Russ. J. Inorg. Chem.* **1982**, *27*, 1722−1724.

10.1021/ic062312u CCC: $37.00
Published on Web 02/17/2007

Its lattice also expands strongly along the hexagonal *c* axis (by ~21%), while it stays nearly unchanged in the basal plane. Its H atom distribution, however, has not been reported yet.

In an attempt to understand better the properties of both hydrides, the Ce_2Ni_7−H system was investigated by a combination of high-resolution synchrotron X-ray diffraction and NPD methods. It will be shown that the system displays preferred hydrogen occupancies in the same structural slabs as in $CeNi_3H_{2.8}$, directional bonding effects, and a new type of structural phase transition in metal−hydrogen systems. Furthermore, in contrast to the analogue lanthanum system La_2Ni_7−H, which remains hexagonal ($La_2Ni_7D_{6.5}$: space group $P6_3/mmc$),[6] the cerium system displays various orthorhombic lattice distortions. Given that these distortions are substantially smaller than those reported for $CeNi_3D_{2.8}$,[3] the structural characterization of this system presented a major challenge.

2. Experimental Part

2.1. Synthesis. Samples of nominal composition Ce_2Ni_7 were prepared by arc-melting cerium (99.93%, Ames Laboratory) and nickel (99.9+%, Alfa) pieces under an argon atmosphere, annealing the ingots at 870 °C for 2 months (quartz tube and 1 bar of argon), and quenching in cold water. Although special protective measures, such as wrapping the intermetallic compound in tantalum foil, were not taken during annealing, no reaction with quartz was observed. X-ray powder diffraction revealed a well-crystallized hexagonal Ce_2Ni_7 phase having cell parameters that did not vary significantly among different samples: $a = 4.93914(18)$ Å, $c = 24.4989(8)$ Å, and $V = 517.58(3)$ Å^3 for the first sample; $a = 4.93847(10)$ Å, $c = 24.4963(4)$ Å, and $V = 517.388(18)$ Å^3 for the second sample. The first sample was subsequently deuterided and characterized with low-temperature NPD. The second sample was fully characterized by X-ray powder diffraction (see the Supporting Information). Rietveld refinement confirmed the structure of Ce_2Ni_7[2] and showed an excellent quality of the sample, which contained 92% of the main phase and 8% of $CeNi_3$. The sample was then split into two parts, so that its hydride and deuteride could be characterized at room temperature with synchrotron diffraction and NPD, respectively.

Deuteration (D_2 gas, 99.8%; AGA) and hydrogenation (H_2 gas, 99.9999%; Alphagas) were carried out in autoclaves at 50−60 °C for 2 days and deuterium/hydrogen pressures of 30−50 bar. Preliminary examination of the reaction products with X-ray powder diffraction showed a uniaxial expansion of the hexagonal cell along the *c* axis, with a cell volume increase of 19−20%. A splitting of some diffraction peaks suggested the presence of a small orthorhombic lattice distortion.

2.2. Synchrotron Powder Diffraction on $Ce_2Ni_7H_x$. The synchrotron experiment was conducted in two stages. First, the Ce_2Ni_7 sample was loaded under 30 bar of hydrogen pressure, taken out of the autoclave, and filled into an open glass capillary. A set of consecutive diffraction patterns was collected shortly after. This in situ experiment was aimed at revealing any possible phase transformation of hydrogenated Ce_2Ni_7 during the release of hydrogen pressure to atmospheric pressure. The measurements started ~5 min after opening of the autoclave and lasted for 6 h. Four consecutive powder patterns were collected for 1.5 h each. The in situ experiment was stopped when virtually no further changes of the diffraction pattern were observed in time. In the second stage, the sample was left in the capillary after the in situ experiment for 3 days to reach a final equilibrium, and an ex situ powder pattern was collected then for 10 h. All measurements were carried out at the high-resolution powder diffraction station BM01B at the Swiss-Norwegian Beam Lines at ESRF: $\lambda = 0.52014(1)$ Å, Debye−Scherrer geometry, 2θ range 1.5−43.5°, step size 0.004°.

2.3. NPD on $Ce_2Ni_7D_x$. Deuterided samples were prepared a few days before the diffraction experiments, examined with X-ray powder diffraction, filled into vanadium containers, and tightly sealed with indium wire. The NPD measurements were performed at the Swiss spallation neutron source SINQ at Paul Scherrer Institut (PSI) in Villigen, Switzerland. One sample was measured at room temperature on HRPT in order to locate the D atoms ($\lambda = 1.49381(2)$ Å, 2θ range 4−164°, step size 0.1°, data collection time 6 h). Another sample was measured at low temperature (1.5−150 K) on DMC in order to check for possible magnetic and structural transitions and to search for a possible increase of the orthorhombic lattice distortion. Fast scans were monitored while cooling the sample from 293 to 1.5 K, and then four patterns were collected at constant temperatures of 1.5, 50, 100, and 150 K ($\lambda = 2.5687(1)$ Å, 2θ range 19−100°, step size 0.1°, data collection time 6 h at 1.5 K and 1.5 h at each of the three other temperatures). Standard NAC and silicon samples were used to calibrate the wavelengths and the diffractometers' zero shifts. Owing to the limited instrumental resolution, the orthorhombic peak splitting was not visually detectable on either one of the two instruments.

3. Structure Determination

3.1. Metal Atom Substructure. The diffraction data of hydrogenated/deuterated Ce_2Ni_7 revealed a strongly anisotropic lattice expansion, with the hexagonal *c* axis increasing by ~21% and the basal plane contracting by −0.8%. Furthermore, the synchrotron ex situ measurements showed peak splitting, corresponding to an orthorhombic distortion of the parent hexagonal lattice. A satisfactory description of this splitting was provided in space group *Cmcm*, a maximal subgroup of $P6_3/mmc$ (symmetry of the hydrogen-free structure). The cell parameter relationships between hexagonal Ce_2Ni_7 (h) and its orthorhombic hydride (o) are $\vec{a}_o = \vec{a}_h$, $\vec{b}_o = \vec{a}_h + 2\vec{b}_h$, and $\vec{c}_o = \vec{c}_h$. Starting from the parent Ce_2Ni_7 structure, a model for the metal atom substructure of the hydride was created in *Cmcm* by using *PowderCell*[7] and refined by the Rietveld method with *FullProf*.[8] A fairly good fit and a reasonable geometry of the metal atom substructure supported this symmetry lowering. However, structure refinements in *Cmcm* revealed the splitting of a Ni atom position located in the middle of the $CeNi_2$ slab. The resulting Ni−Ni dumbbells were aligned along the *c* axis, showed an occupancy of ~50%, and displayed unreasonably short distances (Ni−Ni ~ 2 Å). This apparent disorder suggested that the symmetry had to be further lowered. An analysis of the group−subgroup relations revealed that only two maxi-

(6) Yartys, V. A.; Riabov, A. B.; Denys, R. V.; Sato, M.; Delaplane, R. G. *J. Alloys Compd.* **2006**, *408−412*, 273−279.

(7) Kraus, W.; Nolze, G. *PowderCell*, version 2.3; Federal Institute for Materials Research and Testing: Berlin, Germany, 1999.

(8) Rodriguez-Carvajal, J. *Fullprof Suite*; LLB Sacley & LCSIM: Rennes, France, 2003.

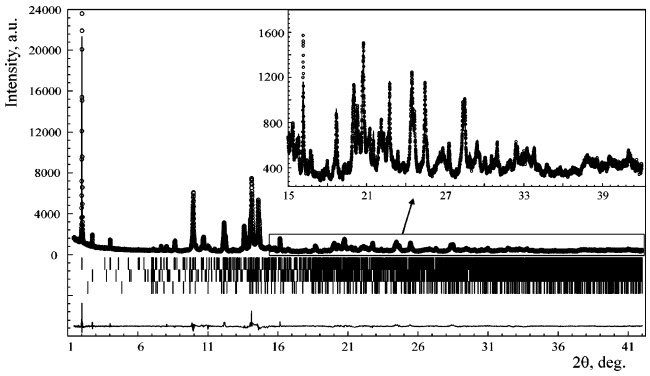

Figure 1. Synchrotron powder diffraction pattern for $Ce_2Ni_7H_x$. Observed (points), calculated (line), and difference (bottom line) patterns are shown. Vertical bars indicate positions of Bragg peaks. The bottom row of vertical bars indicates Bragg positions of the secondary phases ($CeNi_3H_{2.8}$ and Ce_2Ni_7).

mal non-isomorphic space groups of *Cmcm* lead to fully ordered structures. These are *Pmcn* and *Pmnm*, both having the same unit cell as *Cmcm*. Indeed, some weak reflections violated the lattice *C* centering. Thus, new structure models were created in *Pmcn* and *Pmnm* by using *PowderCell*[7] and tested against the data. The fits of both models were satisfactory, but that of *Pmcn* was slightly better. Consequently, the latter space group was retained and later confirmed by successfully locating the D atoms from the NPD data (see section 3.3).

For the $Ce_2Ni_7H_x$ phase, 33 coordinates (4 Ce + 11 Ni atoms) and 3 atomic displacement parameters were refined, including a common displacement parameter for the two Ce sites and the Ni atom site in the $CeNi_2$ slab, another for the remaining two Ce sites, and a third for the remaining 10 Ni sites. In addition, ~5% of $CeNi_3H_{2.8}$ and traces of unreacted Ce_2Ni_7 were included as secondary phases in the refinement. The background was described by a Fourier-filtered smooth function. The final refinement on the synchrotron data in space group *Pmcn* gave the following cell parameters and agreement indices: $a = 4.87726(12)$ Å, $b = 8.5291(2)$ Å, $c = 29.6257(8)$ Å, $V = 1232.40(5)$ Å^3, $R_B = 0.097$, $R_F = 0.101$, $\chi^2 = 8.55$, $R_p = 0.183$, $R_{wp} = 0.177$, 3579 "independent" reflections, and 358 "effective" (accounting resolution)[8] reflections. The observed, calculated, and difference patterns are shown in Figure 1.

3.2. Structural Phase Transition. The intensity profile of the in situ synchrotron data taken on a sample freshly charged with 30 bar of hydrogen pressure changed slowly with time. The first pattern was successfully modeled with a single $Ce_2Ni_7H_x$ phase having the same metal atom arrangement as that determined from the ex situ data (see the previous section). However, its cell parameters were significantly different. While the *c* parameter and the cell volume were very close to those listed in section 3.1, the *a* and *b* parameters indicated a different type of orthorhombic distortion, $\delta = (b/\sqrt{3} - a)/a$, of the parent hexagonal structure. While δ was positive for the ex situ synchrotron data ($\delta = +0.96\%$), it was negative for the in situ data ($\delta = -0.67\%$). The second and third data sets suggested a mixture between two $Ce_2Ni_7H_x$ phases having opposite signs of δ (see Figure 2). The fourth pattern displayed an almost pure

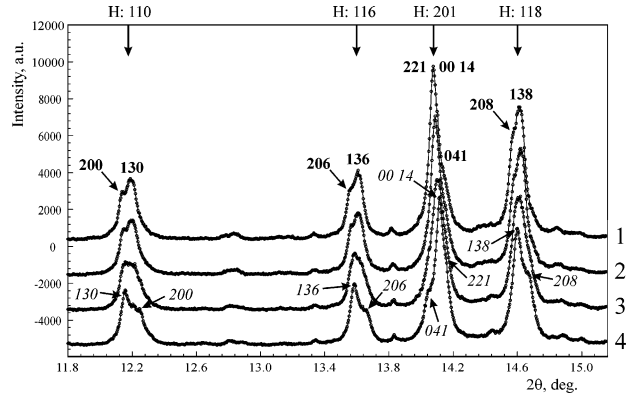

Figure 2. Fragments of the in situ synchrotron powder diffraction patterns collected on the $Ce_2Ni_7H_x$ sample freshly charged with 30 bar of hydrogen. The phase having a negative δ (pattern 1; Laue indices in bold) transforms with time into a phase having a positive δ (pattern 4; Laue indices in italics). Two-phase mixtures are observed on patterns 2 and 3. Laue indices for the average hexagonal structure (H) are indicated on the top of the diagram.

Table 1. Cell Parameters and Orthorhombic Lattice Distortions, δ, of $Ce_2Ni_7H_x$ Constituting the Majority Phase in Each of the Four Consecutively Measured in Situ Synchrotron Powder Diffraction Patterns

pattern no.	*a*, Å	*b*, Å	*c*, Å	*V*, Å^3	δ,[a] %
1	4.92041(13)	8.4650(2)	29.7033(7)	1237.18(5)	−0.67
2	4.91840(15)	8.4618(2)	29.6753(7)	1235.04(6)	−0.67
3	4.88077(14)	8.5219(2)	29.6523(6)	1233.34(5)	+0.81
4	4.87688(10)	8.52590(17)	29.6322(6)	1232.10(4)	+0.93

[a] Degree of orthorhombic distortion defined as $\delta = (b/\sqrt{3} - a)/a$.

phase with $\delta = +0.93\%$, very close to that found in the ex situ data. It is important to note that the whole set of in situ data 1−4 could not be modeled in a satisfactory manner with a single $Ce_2Ni_7H_x$ phase, even if variable degrees of orthorhombic distortion δ were assumed. Cell parameters of the majority of the $Ce_2Ni_7H_x$ phases apparent in each of the four in situ patterns are listed in Table 1.

3.3. Determination of D Atom Positions from NPD. Because of the intrinsically limited resolution of the NPD data, the orthorhombic distortion in $Ce_2Ni_7D_x$ did not show up as individual peak splittings as in the synchrotron data but appeared as a complex peaks' profile. Therefore, the D atom positions (which presumably break the hexagonal symmetry of the structure and induce the orthorhombic distortion) had to be located ab initio by FOX.[9] This program uses global optimization algorithms to solve a structure by trial and error in direct space. The starting models were based on the orthorhombic space groups *Pmcn* and *Pmnm* and the corresponding metal atom positions derived from the synchrotron data and augmented by using the NPD data as collected on HRPT. Reasonably good solutions were obtained in both space groups. However, only *Pmcn* allowed all D atoms to be located on difference nuclear density maps and the entire structure to be refined in a satisfactory manner by the Rietveld method.[8] In total, eight D atom positions were identified, of which two were partially occupied. The refined deuterium content of this phase corresponds to the formula

(9) Favre-Nicolin, V.; Cerný, R. *J. Appl. Crystallogr.* **2002**, *35*, 734−743.

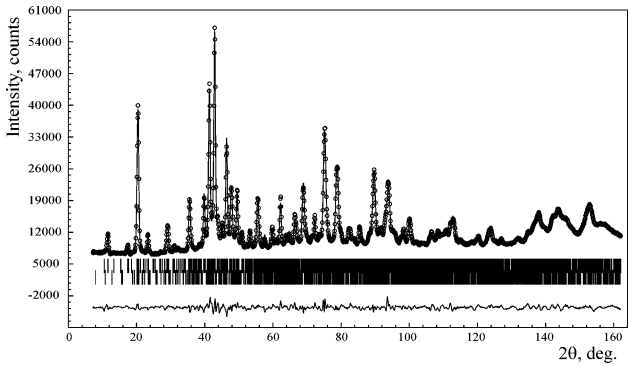

Figure 3. Observed (points), calculated (line), and difference (bottom line) NPD patterns for the $Ce_2Ni_7D_{\sim4}$ sample. The bottom row of vertical bars indicates Bragg positions of the secondary phase ($CeNi_3D_{2.8}$).

$Ce_2Ni_7D_{4.11(4)}$ (see section 4.1) and will be referred to by $Ce_2Ni_7D_{\sim4}$ hereon.

For the $Ce_2Ni_7D_{\sim4}$ phase, 50 atomic coordinates (4 Ce + 11 Ni + 8 D) and 6 atomic displacement parameters were refined, one for the two Ce sites in the $CeNi_2$ slab, another for the remaining two Ce sites, one for the Ni site in the $CeNi_2$ slab, one for the remaining 10 Ni atoms, one for the D atoms belonging to tetrahedral NiD_4 groups (see section 4.2), and one for the remaining D atoms. A secondary phase of composition $CeNi_3D_{2.8}$ (~5 wt %) was modeled by refining a scale factor only. The background was described by 12 points. The final refinement on the HRPT data in space group *Pmcn* resulted in the following cell parameters and agreement indices: $a = 4.8845(3)$ Å, $b = 8.5069(6)$ Å, $c = 29.6073(17)$ Å, $V = 1230.25(14)$ Å^3, $R_B = 0.028$, $R_F = 0.016$, $\chi^2 = 11.1$, $R_p = 0.063$, $R_{wp} = 0.071$, 2892 "independent" reflections, and 182 "effective" (accounting resolution)[8] reflections. The observed, calculated, and difference patterns are shown in Figure 3.

While the diffraction intensities were successfully resolved using the profile information during the Rietveld refinement, strong parameter correlations complicated the elucidation of those structural details that violated hexagonal symmetry. This explains the somewhat higher uncertainties in the D atoms' positions as compared to other accurate NPD experiments (for example, see ref [10]) in spite of the fact that a very good fit to the data has been achieved. The refined cell parameters converged well at an orthorhombic distortion of $\delta = +0.55\%$. Although the absolute value of δ could be slightly underestimated because of the high correlations, the fact that δ is positive is beyond any doubt and in agreement with the ex situ synchrotron diffraction study. It is interesting to note that the orthorhombic distortion in $CeNi_3D_{2.8}$ ($\delta = +1.37\%$) has the same sign and is almost 3 times bigger than that in $Ce_2Ni_7D_{\sim4}$. Clearly, at such large distortions, the positions of the D atoms can be determined more precisely and/or more easily.

3.4. Low-Temperature Behavior of $Ce_2Ni_7D_{\sim4}$ As Studied by NPD. Given that the samples used in the ex situ diffraction studies consisted of a single $Ce_2Ni_7H(D)_x$ phase with orthorhombic distortions smaller than $\delta = \sim+1\%$ (see sections 3.1−3.3), a low-temperature NPD study was aimed at finding conditions under which the positive distortion becomes possibly more pronounced. Unfortunately, the sample cooling did not increase δ in a notable manner. Because the peak splitting was not resolved, the cell parameters at low temperatures were refined in the approximation of a pseudohexagonal lattice (Table 2). The thermal cell expansion was nearly isotropic, and neither magnetic nor structural transitions were detected down to 1.5 K.

Table 2. Parameters of the Pseudohexagonal Unit Cell, Refined for the $Ce_2Ni_7D_{\sim4}$ Structure from the Low-Temperature NPD Data

T, K	*a*, Å	*c*, Å	*V*, Å^3
1.5	4.8917(3)	29.612(4)	613.63(10)
50	4.8918(3)	29.614(4)	613.72(10)
100	4.8927(3)	29.622(4)	614.09(10)
150	4.8948(3)	29.632(4)	614.84(10)

4. Results and Discussion

4.1. Environment of D Atom Sites and Comparison with $CeNi_3D_{2.8}$ and $La_2Ni_7D_{6.5}$. Similar to $CeNi_3D_{2.8}$[3] and $La_2Ni_7D_{6.5}$,[6] the D atoms in $Ce_2Ni_7D_{\sim4}$ are located either in the $CeNi_2$ slab or on the boundary of the $CeNi_2$ and $CeNi_5$ slabs. With respect to their metal atom environment and location in the structure, the fully occupied D1−D6 sites are practically identical to the D1−D6 sites in $CeNi_3D_{2.8}$. However, the partially occupied D7 and D8 sites are different from those in $CeNi_3D_{2.8}$. Metal−deuterium distances within the D atoms' coordination polyhedra of $Ce_2Ni_7D_{\sim4}$ are listed in Table 3. A concise description of the D atom sites and their comparison with those in the related structures is given as follows:

(i) The D1 site is located within a Ce_3Ni_3 antiprism, originating from a D-induced deformation of a Ni_4 site in the parent Ce_2Ni_7 structure. It is equivalent to the D1 sites in $CeNi_3D_{2.8}$ and $La_2Ni_7D_{6.5}$.

(ii) The D2 site is located within another Ce_3Ni_3 antiprism, originating from a D-induced deformation of a $CeNi_3$ site in the parent Ce_2Ni_7 structure. It is equivalent to the D2 sites in $CeNi_3D_{2.8}$ and $La_2Ni_7D_{6.5}$.

(iii) The D3 site is located within a Ce_3Ni tetrahedron, a new interstice formed by a strong D-induced expansion of the $CeNi_2$ slab. It is equivalent to the D3 site in $CeNi_3D_{2.8}$ and to the half-occupied D3 site in $La_2Ni_7D_{6.5}$.

(iv) The D4 site is located within a Ce_2Ni_2 tetrahedron, an interstice existing in the parent Ce_2Ni_7 structure. It is equivalent to the D4 site in $CeNi_3D_{2.8}$ and similar to the D4 site in $La_2Ni_7D_{6.5}$. It is remarkable that the D4 sites in $Ce_2Ni_7D_{\sim4}$ and $CeNi_3D_{2.8}$ provide 0.65−0.75 D atoms per Ce atom of the $CeNi_2$ slab, while the high-multiplicity D4 site in the hexagonal lanthanum analogue $La_2Ni_7D_{6.5}$ provides 3 D atoms per La atom of the $LaNi_2$ slab.

(v) The D5 site is located within a Ce_3Ni tetrahedron, a new interstice formed by a strong D-induced expansion of the $CeNi_2$ slab. It is equivalent to the D5 site in $CeNi_3D_{2.8}$ and to the D3 site in $La_2Ni_7D_{6.5}$.

(vi) The D6 site is located within a Ni_4 tetrahedron, an interstice existing in the parent Ce_2Ni_7 structure. It is

(10) Filinchuk, Y. E.; Sheptyakov, D.; Yvon, K. *J. Alloys Compd.* **2006**, *413*, 106−113.

Table 3. Selected Interatomic Distances (Å) and Angles (deg) in $Ce_2Ni_7D_{\sim4}$ from NPD Data

D atoms' environment				Ni atoms' environment	
D1−Ce1	2.98(3) × 2	D5−Ce1	2.55(4)	Ni1−D3	1.56(4)
D1−Ce2	2.56(5)	D5−Ce2	2.61(4)	Ni1−D5	1.89(2) × 2
D1−Ni8	1.83(3)	D5−Ce2	2.31(4)	Ni1−D6	1.72(3)
D1−Ni10	1.65(2) × 2	D5−Ni1	1.89(2)	D3−Ni1−D5	101(2) × 2
D2−Ce1	2.84(5)	D6−Ni1	1.72(3)	D3−Ni1−D6	128(3)
D2−Ce2	2.78(2) × 2	D6−Ni9	1.64(3)	D5−Ni1−D5	76.7(16)
D2−Ni9	1.63(3)	D6−Ni11	1.82(3) ×2	D5−Ni1−D6	119(2) × 2
D2−Ni10	1.828(17) × 2	D7−Ce1	2.47(4)	Ni8−D1	1.83(3)
D3−Ce1	2.705(18) × 2	D7−Ce2	2.48(5)	Ni9−D2	1.63(3)
D3−Ce1	2.07(5)	D7−Ni1	2.584(11) × 2	Ni9−D6	1.64(3)
D3−Ni1	1.56(4)	D7−Ni11	2.48(3) × 2	Ni10−D1	1.650(20)
D4−Ce1	2.03(4)	D8−Ce2	2.40(6)	Ni10−D2	1.828(17)
D4−Ce3	2.53(4)	D8−Ce4	2.70(5)	Ni10−D4	1.719(15)
D4−Ni10	1.719(15) × 2	D8−Ni11	1.38(2) × 2	Ni11−D6	1.82(3)
				Ni11−D8	1.38(2)

equivalent to the D6 site in $CeNi_3D_{2.8}$ and has no analogue in $La_2Ni_7D_{6.5}$.

(vii) The partially occupied D7 site has an irregular coordination polyhedron made of two close Ce atoms and four distant Ni atoms. It has no analogues in $CeNi_3D_{2.8}$ and $La_2Ni_7D_{6.5}$. As to the D7 site in $CeNi_3D_{2.8}$, its environment consists of two Ce atoms and one Ni atom.

(viii) The partially occupied D8 site is located within a Ce_2Ni_2 tetrahedron, an interstice existing in the parent Ce_2Ni_7 structure. It is similar, although not equivalent, to the D8 site in $CeNi_3D_{2.8}$ and to the D4 site in $La_2Ni_7D_{6.5}$.

The partial occupancy observed for the two latter D sites is consistent with the observed decrease in the cell volume (Table 1) because the H-loaded Ce_2Ni_7 sample was kept under ambient conditions. The volume contraction is presumably due to hydrogen desorption from the D7 and D8 sites. Because there are no short contacts between these partially occupied sites, they can possibly be fully populated and depopulated. This corresponds to the possible compositional range $Ce_2Ni_7D_{3.5-4.5}$ as compared to the refined composition $Ce_2Ni_7D_{4.11(4)}$. The shortest D−D distance is D2−D4 = 1.87(3) Å; all other D−D distances are longer than 2.1 Å.

4.2. Anisotropic Lattice Expansion and Formation of Tetrahedral NiD_4 Units. The cerium compounds $Ce_2Ni_7D_{\sim4}$ and $CeNi_3D_{2.8}$ and the lanthanum compound $La_2Ni_7D_6$ all show anomalous lattice expansions along the hexagonal axes of their respective D-free compounds ($\Delta c/c = \sim20-21\%$ for $Ce_2Ni_7D_{\sim4}$ and $La_2Ni_7D_{6.5}$ and ∼30% for $CeNi_3D_{2.8}$), while their basal planes remain nearly unchanged. In all three structures, deuterium enters the $MgCu_2$-type slabs only, while the bulk of the $CaCu_5$-type slabs remains empty. Consequently, the relative expansion of the $MgCu_2$-type slabs along the *c* axis is considerable and reaches ∼60% in $Ce_2Ni_7D_4$. However, because the $CeNi_5$ slab is nearly unchanged, the total volume expansion of the structure amounts only to $\Delta V/V = \sim19\%$. Although this value is lower than that reported for other Ce-containing deuterides such as $CeMn_{1.8}Al_{0.2}H_{4.4}$ ($\Delta V/V = \sim43\%$),[11] the volume expansion per D atom sets a new record for metal hydrides: 5.95 $Å^3$ per D atom in $Ce_2Ni_7D_{4.11}$, as compared to 5.75 $Å^3$ per D atom in $CeNi_3D_{2.77}$.[3]

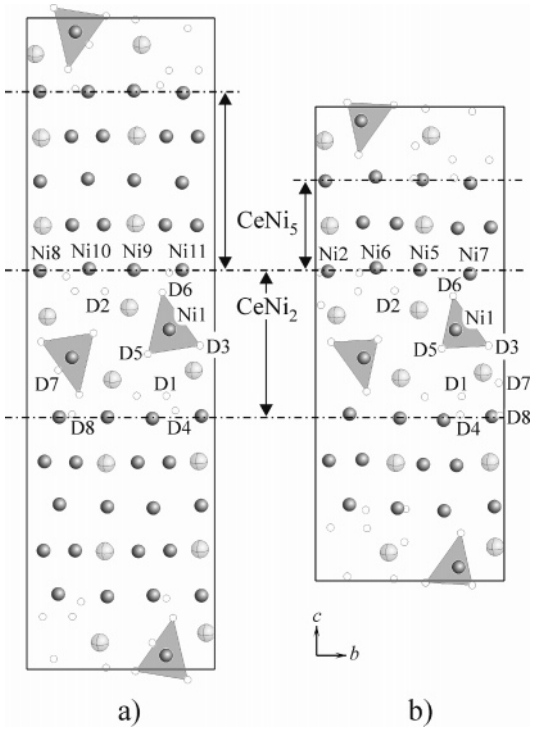

Figure 4. Crystal structure of $Ce_2Ni_7D_{\sim4}$ with $\delta > 0$ (a) and $CeNi_3D_{2.8}$ (b). Atom labels are shown only for D atoms and D-bonded Ni atoms; tetrahedral NiD_4 units are highlighted.

An inspection of the D atom environment around nickel reveals a remarkable feature: as shown in Figure 4a, the Ni atoms located in the center of the $CeNi_2$ slab (Ni1) in $Ce_2Ni_7D_{\sim4}$ are surrounded by four fully occupied D sites (D3, two D5, and D6) in a deformed tetrahedral configuration. Similar tetrahedral NiD_4 units also occur in the $CeNi_2$ slab of $CeNi_3D_{2.8}$ (see Figure 4b). They display Ni−D bond lengths and D−Ni−D bond angles in the ranges 1.56−1.89 Å and 77−128°, respectively, for $Ce_2Ni_7D_{\sim4}$ and 1.50−1.65 Å and 91−122°, respectively, for $CeNi_3D_{2.8}$. The units are reminiscent of the $[NiH_4]^{4-}$ complexes as found in transition-metal hydrides such as

(11) Filinchuk, Y. E.; Sheptyakov, D.; Hilscher, G.; Yvon, K. *J. Alloys Compd.* **2003**, *356−357*, 673−678.

Mg_2NiH_4, $CaMgNiH_4$,[12] $LaMg_2NiH_7$,[13] and $La_2MgNi_2H_8$[14] and thus suggest the presence of directional-bonding effects. Among these hydrides, some derive from intermetallic compounds (Mg_2Ni, $LaMg_2Ni$, and La_2MgNi_2) and are of interest because of their hydrogenation-induced metal−insulator transitions.[14,15]

Hydrogenation-induced symmetry-breaking and directional-bonding effects also occur in the $HoNi_3-D_2$[10] and $ErNi_3-D_2$[16] systems, whose rhombohedral parent structures are quite similar to those of Ce_2Ni_7 and $CeNi_3$. At low deuterium pressure, $HoNi_3$ and $ErNi_3$ form D-poor β_1 phases, which have a lower symmetry than the corresponding intermetallic compounds and, in contrast to $Ce_2Ni_7D_{\sim4}$, contain ordered pyramidal NiD_3 units rather than tetrahedral NiD_4 units within the RNi_2 slabs. Tetrahedral NiD_4 units possibly form in the $ErNi_3-D_2$ system only at relatively high deuterium pressure.[16] It is striking that only the RNi_2 slabs expand in these structures and that the expansion occurs exclusively along the hexagonal *c* axis. Although the expansion is relatively small ($\Delta c/c = \sim14\%$), the structural changes are very similar to those observed in $Ce_2Ni_7D_{\sim4}$ and $CeNi_3D_{2.8}$, especially at low D contents of ∼1.3 D atoms per RNi_3 formula. The tetrahedral NiD_4 units do not break the symmetry further but order within the rhombohedral cell in a parallel orientation. Note in $Ce_2Ni_7D_{\sim4}$ and $CeNi_3D_{2.8}$ that these units order in an antiparallel orientation (Figure 4).

Finally, in $Ce_2Ni_7D_{\sim4}$ only 5 out of 11 Ni sites have D atoms among their nearest neighbors (see Table 3). In contrast to the site forming tetrahedral NiD_4 units (Ni1), the other sites (Ni8−Ni11) are located on the boundary between the $CeNi_2$ and $CeNi_5$ slabs. Similar D-site preferences are also observed for $CeNi_3D_{2.8}$ (see Figure 4). Interestingly, the structural similarity between $Ce_2Ni_7D_{\sim4}$ and $CeNi_3D_{2.8}$ also extends to their hydrogen sorption properties. Despite their different chemical compositions, both compounds have very similar plateau pressures (respectively 0.2 and 0.1 bar at 50 °C). Taken together, these structural findings not only provide further evidence for directional-bonding effects in hydrides that are traditionally considered as "interstitial"[10] but also suggest that the thermal stability of metal hydrides having composite crystal structures can be correlated with metal−hydrogen bond formation/breaking in specific structural units. Clearly, more structure work is necessary to put such correlations on firmer grounds. As to theoretical calculations, they are also desirable but exceedingly difficult to perform at the level of accuracy required for explaining thermodynamic properties, given the structural complexity and disorder of the metal−hydrogen systems involved.

4.3. Anti-isostructural Phase Transition. The structural phase transition observed during the release of hydrogen pressure over the $Ce_2Ni_7H_x$ sample (see sections 2.2 and 3.2) involves two orthorhombic phases. Both derive from the same hexagonal structure and have the same space group symmetry but display different orthorhombic distortions, δ. At high pressure, the $Ce_2Ni_7H_x$ phase has a negative distortion ($\delta < 0$). Upon pressure release, it transforms via a two-phase region into another phase having a positive distortion ($\delta > 0$). This situation is typical for a so-called anti-isostructural phase transition, in which δ is considered as a measure of an order parameter (ref 17 and references cited therein). The existence of such a transition has important implications. Using Landau theory, it was shown[17] that it implies the existence of a third phase having higher symmetry, called a parent phase. Provided that the transitions are not reconstructive, the symmetry of the parent phase corresponds generally to a supergroup of the two low-symmetry structures and, with a few exceptions, that phase is more stable at higher temperatures. The generic phase diagram predicts a first-order transition between the two low-symmetry anti-isostructural phases (which we actually observed) as well as first-order transitions between the high- and low-symmetry phases.[17] This means that under certain pressure and temperature conditions one should be able to remove the orthorhombic distortion altogether, thus stabilizing a disordered hexagonal $Ce_2Ni_7H_x$ structure having $P6_3/mmc$ symmetry. Unfortunately, the phenomenological theory neither allows one to predict the exact conditions under which the parent phase should be stable nor says whether these conditions are achievable, i.e., whether the pressure and temperature assume positive values. Experimentally, pressure and temperature variations can be simulated to a certain degree by isomorphous chemical replacement. Thus, at some level of compositional substitution, compatible with the stability of the $Ce_2Ni_7D_{\sim4}$ structure, a truly hexagonal hydride structure might exist. The $La_2Ni_7D_{6.5}$ structure, reported to have a parent hexagonal symmetry,[6] may be a good candidate for such a parent phase.

According to the above considerations, the tetrahedral NiD_4 units in the parent phase of $Ce_2Ni_7D_x$ are expected to be disordered. A question that remains open is whether these units change orientation as one passes from one low-symmetry phase to another. Given that the structure data reported here concern only one of the phases (that showing a positive distortion, $\delta > 0$), in situ NPD measurements on the other phase (that showing a negative distortion, $\delta < 0$) are required. Such an experiment is feasible because it requires only relatively moderate deuterium pressures (∼30 bar; see section 2.2) but needs considerable further investment. Another way to answer this question would be to investigate similar systems, such as $SmRu_3-H$, and its substitutional derivatives, which were reported to crystallize with the $CeNi_3D_{2.8}$-type structure.[18] Hydrogenation of a Co-

(12) Yvon, K.; Renaudin, G. Hydrides: Solid State Transition Metal Complexes. *Encyclopedia of Inorganic Chemistry*, 2nd ed.; John Wiley & Sons Ltd.: New York, 2005.
(13) Renaudin, G.; Guénée, L.; Yvon, K. *J. Alloys Compd.* **2003**, *350*, 145−150.
(14) Chotard, J.-N.; Filinchuk, Y.; Revaz, B.; Yvon, K. *Angew. Chem., Int. Ed.* **2006**, *45*, 7770−7773.
(15) Yvon, K.; Renaudin, G.; Wie, C. M.; Chou, M. Y. *Phys. Rev. Lett.* **2005**, *94*, 066403.
(16) Filinchuk, Y. E.; Yvon, K. *J. Alloys Compd.* **2005**, *404−406*, 89−94.
(17) Tolédano, P.; Dmitriev, V. *Reconstructive phase transitions: in crystals and quasicrystals*; World Scientific: London, 1996.
(18) Shilov, A. L.; Iaropolova, E. I.; Kost, M. E. *Dokl. Akad. Nauk SSSR* **1980**, *252*, 1397−1400 (in Russian).

substituted $SmRu_3$, for example, results in an orthorhombically distorted hydride with $\delta = \sim+2.2\%$, while a Ni-substituted analogue forms a hydride with $\delta = \sim-4.7\%$. Thus, anti-isostructural phase transitions may be a relatively general phenomenon in such types of metal−hydrogen systems.

Acknowledgment. This work was supported by the Swiss National Science Foundation and the Swiss Federal Office of Energy and was partially performed at the Swiss Spallation Neutron Source SINQ at PSI, Villigen, Switzerland. The help of Denis Sheptyakov (PSI) in particular is acknowledged. Y.E.F. thanks Vladimir Dmitriev (SNBL at ESRF) for useful discussions.

Supporting Information Available: Structural data as CIF files. This material is available free of charge via the Internet at http://pubs.acs.org.

IC062312U